

EFFECT OF Na₂CO₃ DEGUMMING CONCENTRATION ON LiBr-FORMIC ACID-SILK FIBROIN SOLUTION PROPERTIES

by

Zhi LIU^a, Yuqin WAN^b, Hao DOU^a, and Ji-Huan HE^{a,c*}

^a National Engineering Laboratory for Modern Silk, College of Textile and Clothing Engineering,
Soochow University, Suzhou, China

^b College of Textiles and Clothing, Jiangnan University, Wuxi, China

^c Nantong Textile Institute, Soochow University, Nantong, China

Original scientific paper
DOI: 10.2298/THSI1603985L

Salt-acid system has been proved to be of high efficiency for silk fibroin dissolution. Using salt-acid system to dissolve silk, native silk fibrils can be preserved in the regenerated solution. Increasing experiments indicate that acquirement of silk fibrils in solution is strongly associated with the degumming process. In this study, the effect of sodium carbonate degumming concentration on solution properties based on lithium bromide-formic acid dissolution system was systematically investigated. Results showed that the morphology transformation of silk fibroin in solution from nanospheres to nanofibrils is determined by sodium carbonate concentration during the degumming process. Solutions containing different silk fibroin structure exhibited different rheological behaviors and different electrospinnability, leading to different electrospun nanofibre properties. The results have guiding significance for preparation and application of silk fibroin solutions.

Key words: biomaterials, degumming, electrospinning, nanofibrils, silk

Introduction

In recent years, due to the urgent demands of bioactive materials, silk-based materials have attracted more attention from many biomedical fields, such as tissue engineering [1], wound dressing [2] and drug release systems [3], for their excellent properties.

Silk consists of two proteins, sericin protein and fibroin protein. For the previous mentioned applications, silk is normally degummed to extract sericin protein. Considering the cost and the efficiency of the process, silk is generally degummed with sodium salts, sodium carbonate (Na₂CO₃) in many cases, in boiling water. As an effective dissolution system of silk fibroin (SF), salt-acid system has been proved a facile step to dissolve SF in the past two years. For instance, SF films prepared from formic acid-hydroxyapatite degumming system were found had higher breaking strength and extension at break [4]; the SF solutions from formic acid/CaCl₂ showed good electrospinn ability and the regenerated nanofibres exhibited high mechanical properties [5]. It has been found that using salt-acid dissolution system is capable of preserve the native silk nanofibrils structure [6]. Increasing experiments show that acquirement of nanofibrils is strongly affected by the degumming process. However, degumming process is

* Corresponding author; e-mail: hejihuan@suda.edu.cn

usually neglected while many researches have been conducted for formation of SF products. As a matter of fact, degummed silk is often purchased from different suppliers for many researches, without known information about the degumming process, which is inappropriate for biomedical applications of silk.

In this paper, we aim to investigate the effect of different Na₂CO₃ degumming concentrations on SF morphology and SF morphology in lithium bromide-formic acid (LiBr/FA) dissolution system. Meanwhile, to further evaluate the effect of Na₂CO₃ degumming concentrations on resultant electrospun SF nanofibre properties. To fulfill these tasks, three typical weight ratio of Na₂CO₃ (0.5 wt.%, 0.05 wt.%, 0.005 wt.%) were prepared for degumming and LiBr/FA system was used to dissolve the degummed silk. Results showed that with varying weight ratio of Na₂CO₃, SF exhibited different morphology after degumming. Under same dissolution system of LiBr/FA, SF morphology changed from nanospheres to nanofibrils in three typical solutions. Subsequently, resultant SF nanofibres mats showed different properties including secondary structure and mechanical properties.

Experimental section

Materials

Raw *B. mori* silk was purchased from Zhejiang Province, China. Anhydrous sodium carbonate, formic acid (98% v/v) and anhydrous lithium bromide were purchased from Sinopharm Chemical Reagent Co., Ltd. (Shanghai, China). All reagents were of analytical grade and were used as received without further treatment.

Degumming and preparation of regenerated silk fibroin (RSF) solutions

The *B. mori* silk was degummed in boiling Na₂CO₃ aqueous solution for 60 minute, with Na₂CO₃ concentration of 0.5 wt.%, 0.05 wt.%, and 0.005 wt.%, respectively. The degummed silk was then rinsed thoroughly with deionized water to remove the sericin protein. The process repeated three times. The degummed silks are named 0.5%-SF, 0.05%-SF, and 0.005%-SF, respectively, with according weight loss of 33.2 ± 1.6%, 28.5 ± 1.3%, 26.8 ± 0.9%.

Table 1. Sample codes of SF and its dissolution parameters

Sample	LiBr [wt.%]	FA [wt.%]	Dissolution time [min]
0.5%-SF	2	98	2
0.05%-SF	2	98	40
0.005%-SF	2	98	300

The weight loss of raw silk after degumming was measured using the following equation: weight loss [%] = (1 – dry mass of degummed silk/dry mass of raw silk) × 100. Five specimens of each sample were test. The degummed silks were directly dissolved in LiBr/FA system at room temperature. Table 1 lists the sample codes and their dissolution parameters.

Preparation of SF films and electrospun SF nanofibres

The 10 wt.% SF concentrations were prepared by dissolving the three typical regenerated films in formic acid (FA) for 3 hours before electrospinning. A high electric potential of 12 kV was applied and the collect distance was 12 cm. A constant volume flow rate of 0.8 ml/h was maintained using a syringe pump. The regenerated SF mats are called 0.5% RSF, 0.05% RSF and 0.005% RSF, respectively. The ambient relative humidity was 50 ± 2 % and the temperature was 25 ± 2 °C.

Measurement and characterization

The morphology of degummed silk and electrospun SF nanofibres was observed using a scanning electron microscope (SEM), Hitachi S-4800, Tokyo, Japan. The diameters of nanofibres were calculated by measuring at least 100 fibers at random using Image J program. Morphology of SF in solution was observed by atomic force microscopy (AFM), Veeco, Nano scope V. To prepare the samples for AFM imaging, SF/FA solutions of 0.001 wt.% were prepared. Then 2 L of the diluted SF/FA solution was dropped onto freshly cleaved mica. Rheological studies were run on a rheometer (AR2000, TA Instruments, and America) with a 40 mm cone plate (Ti, 40/2°). The secondary structure of SF nanofibre mats was measured by fourier transform infrared (FTIR) spectroscopy on Nicolet5700 (Thermal Nicolet Company, USA). The X-ray diffraction (XRD), X Pert Pro MPD, PANalytical, The Netherlands, was operated at 40 kV tube voltages and 40 mA tube current. The mechanical properties of electrospun SF nanofibre mats (10 mm × 40 mm) were obtained using a universal testing machine (model 3365 electronic strength tester, Instron, Boston, USA), gauge length: 20 mm; cross-head speed: 0.2 mm/s at 25 ± 0.5 °C, 60 ± 5% relative humidity. The thickness of the mats was measured using a micrometer.

Results and discussion

Morphology of degummed silk at micro scale

It can be clearly seen that morphology of SF varies if the weight ratio of Na₂CO₃ changes, fig. 1. For raw silk, sericin protein entirely covers the surface of fiber so that no SF can be seen. Residual sericin was also observed for 0.005%-SF since the dose of Na₂CO₃ was not enough to extract sericin completely. For 0.05%-SF, sericin nearly disappeared, indicating well removal of sericin. As the concentration of Na₂CO₃ further increased (0.5%-SF), sericin completely disappeared and nanopores were observed, suggesting the adverse effect on SF due to overdose of Na₂CO₃. The observations were confirmed by the weight loss of silk after degumming. For 0.5%-SF, a weight loss of 33.2 ± 1.6% was measured indicating damage of SF structure.

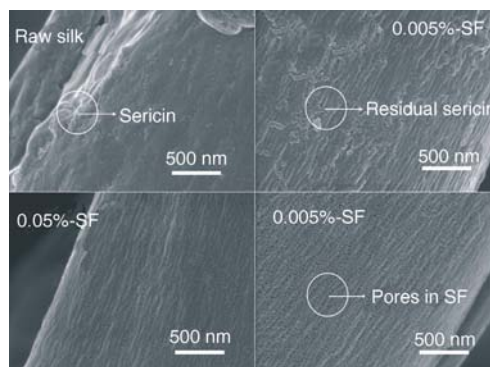


Figure 1. The SF morphology at micro scale at different Na₂CO₃ degumming concentrations

Solution behavior of SF solutions

The dissolution behavior of regenerated solutions

Significantly different dissolution behaviors were observed under same dissolution system of LiBr/FA, as shown in tab. 1 and fig. 2. The dissolution times varied and the color of regenerated solutions were different. In fact, 0.5%-SF dissolved rapidly as soon as SF contacted the solvent as LiBr/FA solvent diffuse

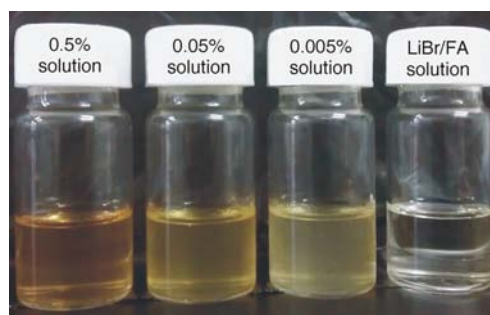


Figure 2. Regenerated solutions under three degummed SF with LiBr/FA solution as comparison

into SF through nano-pores quickly, subsequently, SF dissolved completely in just a few minutes due to the strong interaction with solvent. On the contrary, the dissolution time of 0.05%-SF and 0.005%-SF were about 40 minute and 300 minute, respectively. The proper dose of Na_2CO_3 made it possible to dissolve SF under a mild process (0.05%-SF). The solution color was golden yellow, which is similar to traditional method (LiBr aqueous solutions and $\text{CaCl}_2/\text{C}_2\text{H}_5\text{OH}/\text{H}_2\text{O}$ solutions) [7]. More time was needed to dissolve 0.005%-SF completely as the residual sericin covered on the surface of SF protecting SF from dissolving. The light yellowish-white color of the regenerated SF solution indicated a weak interaction between SF and solvent. The huge difference of dissolution behaviors suggests that the weight ratio of Na_2CO_3 has significant effect on degummed SF and regenerated solution properties.

Rheological behavior of regenerated solutions

To reveal the Na_2CO_3 degumming concentrations effect on the solution properties, rheological behavior of three typical solutions and morphology of SF in regenerated solutions were investigated. As shown in fig. 3(a), the 0.5% solution showed Newtonian fluids with low viscosity, but the 0.05% and 0.005% solutions with higher viscosities exhibited shear-thickening behavior followed by shear-thinning, which is similar to natural silk dope [8]. As shown in fig. 3(b), nanospheres were observed in 0.5% solution which indicates that the SF is likely decomposed to macromolecules level during the dissolving process. In the 0.05% solution, native silk nanofibrils

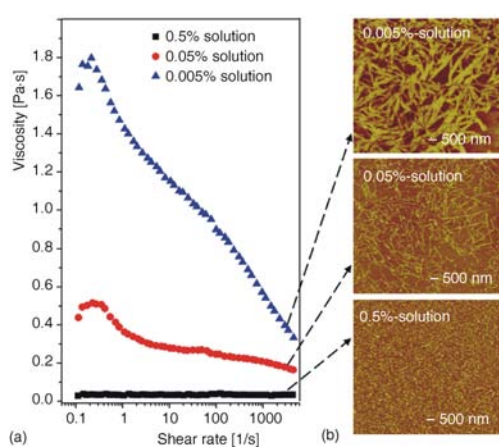


Figure 3. (a) rheological behaviors of regenerated solutions, (b) morphology of SF in regenerated solutions accordingly

with diameter of about 20-40 nm were preserved through the mild process using LiBr/FA solvent, fig. 3(b). When shearing at low shear rates, the nanofibrils entangled with each other, resulting in the increased viscosities and shear-thickening behavior. The subsequent shear-thinning behavior observed at high shear rates is likely due to the orientation of the nanofibrils. In 0.005% solution, nanofibrils with diameters of about 40-80 nm were observed, fig. 3(b). The higher diameter strengthened the entanglement and friction when shearing, favoring higher viscosity than 0.05% solution, fig. 3(a). Meanwhile, residual sericin physically adhered to the SF nanofibrils, resulting in larger silk aggregates (sericin aggregates, SF nanofibrils aggregates, sericin-SF nanofibrils aggregates). As a result, higher viscosity was obtained.

Properties of RSF nanofibres mat

Morphology of as-spun SF nanofibres mat

To further evaluate the processability of SF solutions under different Na_2CO_3 degumming concentrations, SF nanofibres were fabricated by electrospinning from 10 wt.% SF/FA solution. The SEM images of the nanofibres are shown in fig. 4. Beaded and non-uniform SF nanofibres obtained from the 0.5% solution showed bad spin-ability. On the contrary, uniform and smooth SF nanofibres, with RSF nanofibres diameter of 232.6–31.1 nm and

423.2 29.4 nm, respectively, were obtained from the 0.05% solution and 0.005% solution, exhibiting good spin-ability of the two solutions. The low viscosity and Newtonian fluids behavior of 0.5% solution means low macromolecule chains entanglements in the solution, therefore it exhibited poor spin-ability and resulted in beaded SF nanofibres. Compared with the 0.5% solution, the 0.05% solution and 0.005% solution exhibited higher viscosities, better spin-ability and yielded uniform SF nanofibres and higher diameter of SF nanofibres. This study is in accordance with previous study, which reported that solution containing self-assemble nanofibres shows better spin-ability in electrospinning process [9]. The different spin-ability of these solutions suggested the important role of silk structure in electrospinning process.

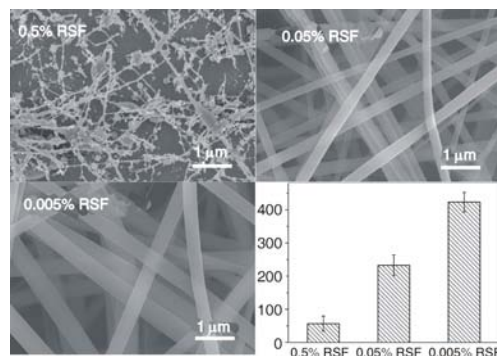


Figure 4. Morphology and diameter of as-spun SF nanofibres mat (0.5% RSF, 0.05% RSF, and 0.005% RSF)

Secondary structure of as-spun SF nanofibres mat

The FTIR and XRD have been used to examine the secondary structure of silk proteins. As shown in fig. 5(a), the absorption peaks of 0.5% RSF and 0.05% RSF are at around 1536 cm⁻¹ (amide II), and the 0.005% RSF is at 1523 cm⁻¹ (amide II), indicating the transition of random coil or helical conformation to β -sheet structure [10]. This structural transition of SF nanofibres was also confirmed by XRD analysis, fig. 5(b). A broad diffraction peak at 20.2° indicates the molecular structure transition from silk I to silk II [10]. These results synergistically demonstrate that the Na₂CO₃ degumming concentration have effect on secondary structure of regenerated electrospun SF nanofibres mat. The residual sericin may contribute to the improvement of crystallinity degree of RSF mat as the 0.005% RSF showed a sharper peak.

Mechanical properties of as-spun SF nanofibres mat

Mechanical properties of as-spun RSF mats were also investigated and the results are shown in fig. 6. As expected, 0.5% RSF mat showed relatively poor mechanical properties with a breaking strength and an extension at break of 2.15 MPa, 4.73%, respectively, tab. 2. And 0.05% RSF mat and 0.005% RSF mat showed

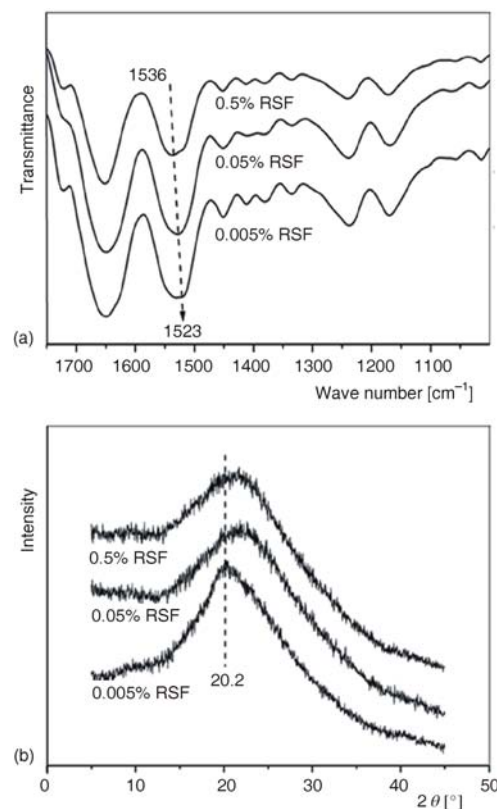


Figure 5. The FTIR and XRD measurements of as-spun SF nanofibres mat

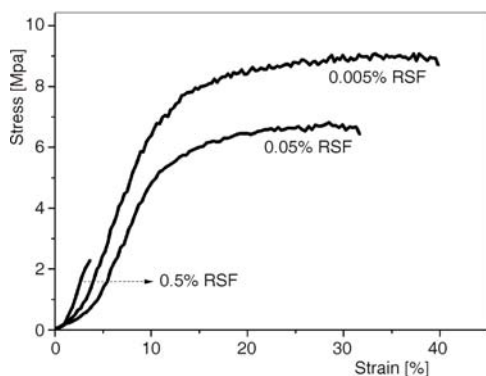


Figure 6. Mechanical properties of as-spun SF nanofibres mat

Table 2. Diameters and mechanical properties of as-spun SF nanofibres mat

RSF sample	Diameter [nm]		Breaking strength [MPa]		Extension [%]	
0.5% RSF	56.7	22.6	2.15	0.43	4.73	0.81
0.05% RSF	232.6	31.1	6.93	0.38	32.65	3.27
0.005% RSF	423.2	29.4	8.63	0.45	40.00	3.75

higher mechanical properties of with breaking strength and extension at break of 6.93 MPa, 32.6%, and 8.63 MPa, 40.0%, respectively, tab. 2. The improvement mechanical properties of the three typical RSF mats might be attributed to

the increased crystallinity, fig. 5. The silk nanofibrils in the solutions also play an important role in improving the mechanical properties of regenerated silk products [11]. These results showed that even with the same dissolution system, different Na₂CO₃ degumming concentrations can lead to remarkably different SF as well as regenerated SF solution behavior, and subsequently dramatically different spin-ability and mechanical properties of RSF product.

Conclusions

The change of SF morphology from nanospheres to nanofibrils was determined by Na₂CO₃ concentration during the degumming process. This study verified three facts:

- Na₂CO₃ weight ratio has great effect on degumming process,
- by altering the Na₂CO₃ degumming concentration, regenerated SF structure can be changed from nanospheres to nanofibrils, and
- the Na₂CO₃ degumming concentration affects the spin-ability of the regenerated SF solution and subsequently, leading to different SF nanofibre mechanical properties. These results will have guiding significance to researchers with respect to silk.

Acknowledgment

The work is supported by Priority Academic Program Development of Jiangsu Higher Education Institutions (PAPD), National Natural Science Foundation of China under Grant No. 11372205 and Grant No. 51203066, Project for Six Kinds of Top Talents in Jiangsu Province under Grant No. ZBZZ-035, and Science & Technology Pillar Program of Jiangsu Province under Grant No. BE2013072.

References

- [1] He, C.-H., et al., Bubble Spinning for Fabrication of PVA Nanofibers, *Thermal Science*, 19 (2015), 2, pp. 743-746
- [2] Vasconcelos, A., et al., Novel Silk Fibroin/Elastin Wound Dressings, *Acta Biomaterialia*, 8 (2012), 8, pp. 3049-3060
- [3] Chen, R., et al., Bubble Rupture in Bubble Electrospinning, *Thermal Science*, 19 (2015), 4, pp. 1141-1149
- [4] Ming, J., et al., Novel Silk Fibroin Films Prepared by Formic Acid/Hydroxyapatite Dissolution Method, *Materials Science and Engineering: C*, 37 (2014), Apr., pp. 48-53
- [5] Liu, Z., et al., Preparation of Electrospun Silk Fibroin Nanofibers from Solutions Containing Native Silk Fibrils, *Journal of Applied Polymer Science*, 132 (2015), 1, p. 41236

- [6] Porter, D., *et al.*, Silk as a Biomimetic Ideal for Structural Polymers, *Advanced Materials*, 21 (2009), 4, pp. 487-492
- [7] Sashina, E. S., *et al.*, Structure and Solubility of Natural Silk Fibroin, *Russian Journal of Applied Chemistry*, 79 (2006), 6, pp. 869-876
- [8] Holland, C., *et al.*, Comparing the Rheology of Native Spider and Silkworm Spinning Dope, *Nature Materials*, 5 (2006), 11, pp. 870-874
- [9] Zhang, F., *et al.*, Mechanisms Control of Silk-Based Electrospinning, *Biomacromolecules*, 13 (2012), 3, pp. 798-804
- [10] Jeong, L., *et al.*, Time-Resolved Structural Investigation of Regenerated Silk Fibroin Nanofibers Treated with Solvent Vapor, *International Journal of Biological Macromolecules*, 38 (2006), 2, pp. 140-144
- [11] Zhang, F., *et al.*, Facile Fabrication of Robust Silk Nanofibril Films via Direct Dissolution of Silk in CaCl₂-Formic Acid Solution, *ACS Applied Materials & Interfaces*, 7 (2015), 5, pp. 3352-3361